1

Introduction

1.1 Background

With ever growing concerns about energy sustainability and environmental issues, the adoption of electric vehicles (EVs) such as pure electric vehicles (PEVs) and plug-in electric vehicles (PHEVs) has been identified to be one of the most effective strategies to reduce dependency on fossil fuels and greenhouse gas emission, and has attracted more and more attention from governments, industries, and customers [1, 2]. Many countries have taken aggressive step to promote EVs to meet emission targets under the Paris climate accord [3]. France has announced its plan to stop selling petrol and diesel-powered cars by 2040. The UK follows France in banning sales of new petrol and diesel cars from 2040. Norway, which has the highest number of EVs in the world, has set a target of only allowing sales of 100% PEVs or PHEVs by 2025. The Netherlands has mooted a 2025 ban for diesel and petrol cars. Germany has passed a resolution calling for a ban on combustion engine cars by 2030. India is mulling the idea of moving toward prohibiting the internal combustion engine in 2030. China is developing a plan to phase out vehicles powered by fossil fuels [4]. Though China has not yet suggested any concrete timeline, it has ambitious goals for automotive efficiency and climate change including a cap on carbon emissions by 2030. Experts suggest this new ban might come into force around then. The policies of restricting sales of diesel and petrol cars in these countries have stimulated carmakers around the world to accelerate the research and development of EV technologies and the commercialization of EVs.

EVs in this book refer to vehicles which are wholly or partially driven by an electric motor using energy stored in batteries. They have merits over internal combustion engine vehicles (ICEVs) in terms of the energy consumed, which can be generated from various energy sources including renewable energy sources (RESs). As the energy of batteries is depleted, they are recharged by the electricity from power grids. In order for EVs to be truly clean and sustainable road transportation, electricity generation needs to come from power grids with the integration of more RESs [5]. However, the intermittent nature of RESs adversely affects power grid voltage, frequency, and reactive power. Such a power grid needs to be compensated by energy storage which stores the excessive power generated from RESs and delivers power back into grids to offset high demand during peak hours [6]. The batteries in EVs are good candidates as energy storage and they can play the role of power compensation which enhances power grid resilience and provides an opportunity for better acceptance of RESs. As such, the batteries in an EV not only provide energy to drive it but also exchange energy with power grids to stabilize

Advanced Battery Management Technologies for Electric Vehicles, First Edition. Rui Xiong and Weixiang Shen.

power systems. In such applications, the batteries operate at dynamic and deep cyclic conditions that can lead to poor performances and premature aging [7, 8]. Advanced battery management technologies (BMTs) are needed to monitor and control the batteries in EVs for performance improvement and life extension. BMTs involve battery modeling, battery states estimation, battery charging, battery balancing, and battery thermal management [9], which will be discussed in the rest of the book. In this chapter, the fundamentals of EVs are first explained. Then, energy and power requirements of batteries in EVs and performances of current battery technologies are discussed. Finally, the key BMTs and the functions of battery management systems (BMSs) will be briefly introduced.

1.2 Electric Vehicle Fundamentals

Depending on the configuration of an EV, the propulsion power and energy of the EV can be partially or wholly supplied by the batteries installed in it. Without loss of generality, a PEV is used as an example to discuss the working principle. Similar to ICEVs, the powertrain in a PEV provides power to move a vehicle and energy to cover a certain driving distance under different road conditions and driving modes [10, 11]. The force that a vehicle must overcome to travel is known as road load. As shown in Figure 1.1, the road load F_L consists of three major components: aerodynamic drag force F_d, rolling resistance force $F_{r,}$ and climbing force F_c as given by

$$F_L = F_d + F_r + F_c \tag{1.1}$$

The aerodynamic drag force is the friction of the vehicle moving through the surrounding air and is expressed as

$$F_d = \rho A C_d (V - V_w)^2/2 \tag{1.2}$$

where ρ is the density of the surrounding air, A is the vehicle frontal area, C_d is the aerodynamic drag coefficient, V is the vehicle speed, V_w is the wind speed in the opposite direction of the moving vehicle, and θ is the angle of the slope.

The rolling resistance force is caused by the deformation of the wheel and road surface. The deformation of the wheel heavily dominates the rolling resistance while the

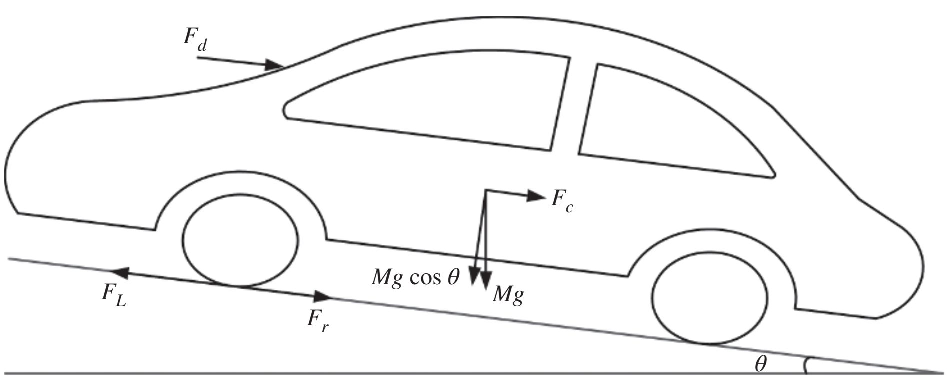

Figure 1.1 Forces applied on a vehicle.

deformation of the road surface is generally insignificant. The rolling resistance force is normally calculated by

$$F_r = MgC_{rr}\cos\theta \tag{1.3}$$

where M is the overall mass of the vehicle, g is the gravitational acceleration, and C_{rr} is the rolling resistance coefficient.

The climbing force is the downward force for a vehicle to climb up a slope which is the resolution of the gravity force due to the vehicle weight that acts along the slope

$$F_c = Mg\sin\theta \tag{1.4}$$

According to Newton's second law, the acceleration of a vehicle is determined by all forces applied on it, which is given by

$$a = (F_t - F_L)/(k_t M) \tag{1.5}$$

where F_t is the total traction force available to overcome the road load F_L and drive the vehicle with the acceleration α, and k_t is the mass factor that converts the rotational inertia of rotating components into equivalent translational mass. As a result, the total propulsion force can be expressed as

$$F_t = k_t M\alpha + F_d + F_r + F_c \tag{1.6}$$

The power demand to drive the vehicle at the speed V can be calculated by

$$P_t = F_t V = k_t M\alpha V + F_d V + F_r V + F_c V \tag{1.7}$$

Correspondingly, the energy required to move the vehicle for a certain distance from time t_0 to t can be calculated by

$$E_t = \int_{t_0}^{t} P_t dt \tag{1.8}$$

Depending on the traction force F_t, the vehicle can operate at three driving modes:

- *Traction mode.* $F_t > 0$, the traction force overcomes road load to move the vehicle forward.
- *Braking mode.* $F_t < 0$, the kinetic energy of the vehicle is dissipated by brakes or regenerative braking, and the propulsion system can either work or be cut off.
- *Coasting mode.* $F_t = 0$, the vehicle propulsion system stops working, and all the kinetic energy is deceased and transformed to the resistance losses.

It should be noted that EV batteries only need to provide energy in the traction mode.

1.3 Requirements for Battery Systems in Electric Vehicles

Three common parameters are normally used to assess EV performance [10]:

- *Range per charge.* This is the driving distance when the batteries in EVs are fully charged. It may vary with the conditions of use and can be determined on the basis of an operation condition of a constant speed on a level road or a type of driving cycle or the loosely defined urban or highway situations. For example, an EV can offer 250 km per charge at a constant speed of 60 km h^{-1} or 170 km per charge under a new European driving cycle (NEDC) combined cycle.

- *Acceleration rate*. This is usually represented by the minimum time required to accelerate the vehicle from zero to specific speeds, such as 40, 60, or 80 km h^{-1}.
- *Maximum speed*. This is the maximum safe speed which the vehicle can attain. It does not mean the speed limit on the public road but mainly indicates vehicle performance.

1.3.1 Range Per Charge

Standard driving cycles are generally used to evaluate the driving range for EVs in different regions and countries [12, 13].

(1) *In the USA*. The Urban Dynamometer Driving Schedule (UDDS) is the most common driving cycle, which is also known as the FTP-72 cycle or LA-4 cycle or Federal Urban Driving Schedule (FUDS). It was developed originally to evaluate the noxious emissions of ICEVs and was based on a cycle derived from the statistical flow of traffic patterns in Los Angeles. Subsequently, it has been widely used to evaluate the fuel economy of urban or city driving. In contrast, the Federal Highway Driving Schedule (FHDS) was developed to represent driving patterns in rural or cross-country conditions. It is also known as The United States Environmental Protection Agency (US EPA) Highway Fuel Economy Test (HWFET) or US EPA HWFET. Figures 1.2 and 1.3 show their corresponding speed–time profiles.

(2) *In Europe*. The ECE-15 cycle was the first driving cycle to be legislated in the European Union. The name ECE-15 corresponds to United Nations Economic Commission for Europe (UNECE) Regulation No. 15 published on April 11, 1969. It was developed to represent the urban driving cycle (UDC), e.g. in Paris or Rome, as shown in Figure 1.4. It is characterized by low vehicle speeds, low engine load, and low exhaust gas temperature. The Extra Urban driving cycle (EUDC) was

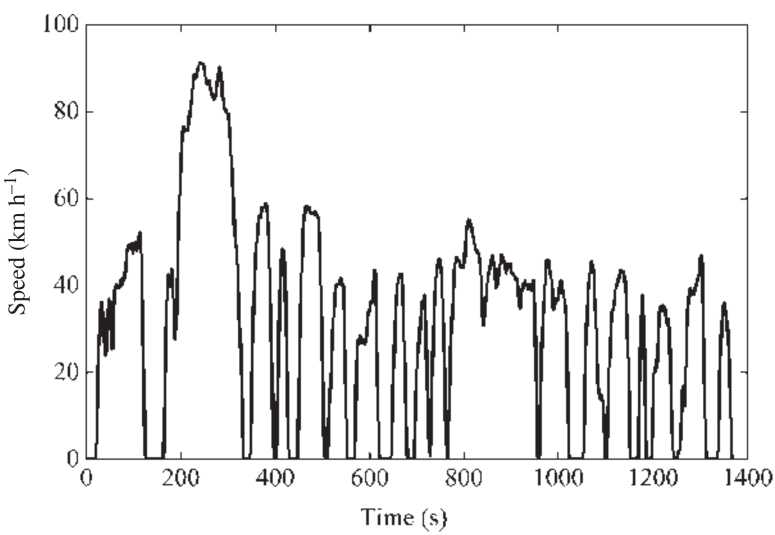

Figure 1.2 Speed versus time under UDDS.

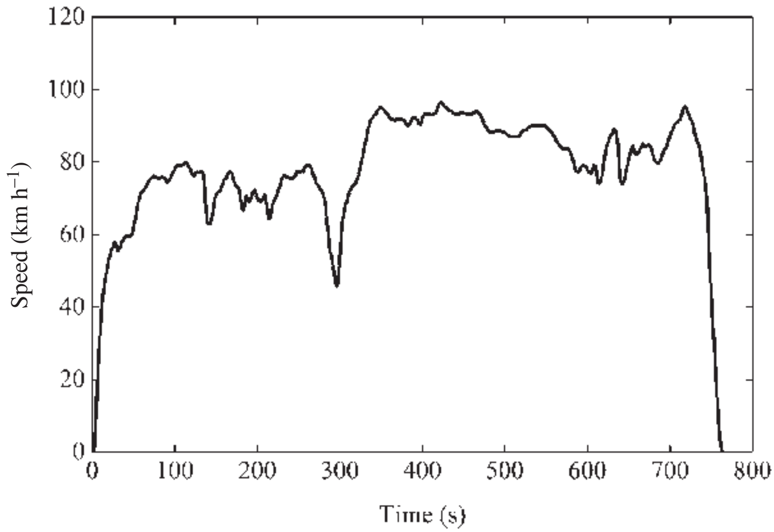

Figure 1.3 Speed versus time under FHDS.

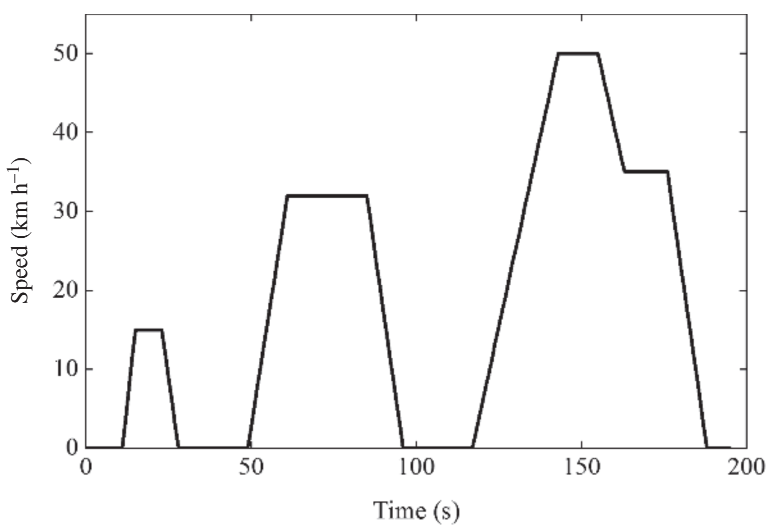

Figure 1.4 Speed versus time under ECE-15.

developed to include more aggressive and high speed driving modes, as shown in Figure 1.5. NEDC is a composite of four repeating ECE-15 cycles and one EUDC, as shown in Figure 1.6. NEDC is widely adopted in Europe to evaluate fuel economy and emissions of ICEVs. It is also adopted to evaluate the driving range and energy consumption of EVs.

(3) *In Japan*. Japanese 10.15 Mode was developed to reflect metropolitan driving conditions as well as highway driving conditions, based on driving performance studies in major cities in Japan. The profile of the Japanese 10.15 Mode is composed of three

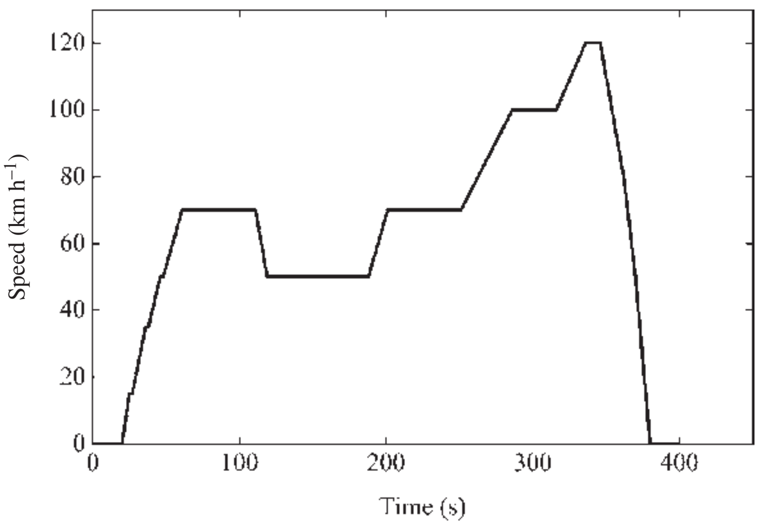

Figure 1.5 Speed versus time under EUDC.

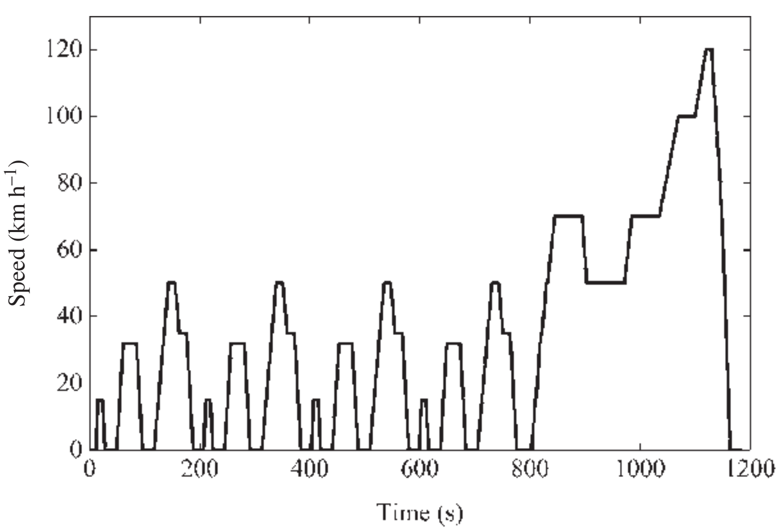

Figure 1.6 Speed versus time under NEDC.

repetitions of J10 followed by J15, as shown in Figure 1.7. As a regulation, the driving range of EVs in Japan is evaluated only by the Japanese 10.15 Mode driving cycle.

To evaluate power and energy requirements for the batteries in EVs under the above standard driving cycles, a typical PEV with the parameters shown in Table 1.1 is taken as an example [5].

When the typical PEV is running in these standard driving cycles, the batteries in it will supply power and energy to vehicle movement as well as auxiliary units. For

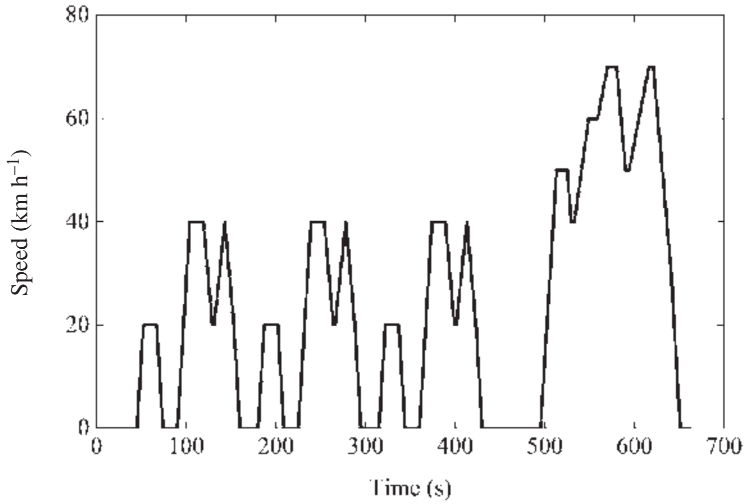

Figure 1.7 Speed versus time under Japanese 10.15 Mode.

Table 1.1 Parameters of a typical PEV.

Mass, M	1360 kg
Mass factor, k_t	1.05
Acceleration rate, 0 to 100 km h^{-1} in 10 s	2.68 m s^{-2}
Coefficient of rolling resistance, C_{rr}	0.01
Air density, ρ	1.225 kg m^{-3}
Vehicle frontal area, A	2 m^2
Aerodynamic drag coefficient, C_d	0.5
Wind speed, V_w	0 m s^{-1}
Road slope angle, θ	0°
Efficiency of gearbox to wheels	1.0
Efficiency of motor to gearbox	0.9
Efficiency of inverter to motor	0.95
Efficiency of batteries to inverter	0.95

simplicity, this book only discusses the energy and power demands of vehicle kinetics and ignores those required by auxiliary units. The five standard driving cycles of UDDS, FHDS, ECE-15, NEDC, and Japanese 10.15 Mode are used to analyze the power and energy demands of this PEV. According to Eq. (1.7), the power demands corresponding to the five standard driving cycles are calculated and their results are shown in Figures 1.8–1.12, respectively.

Since the batteries provide energy to drive the EV only in the traction mode, the energy demands in the traction mode are calculated under the five standard driving cycles by

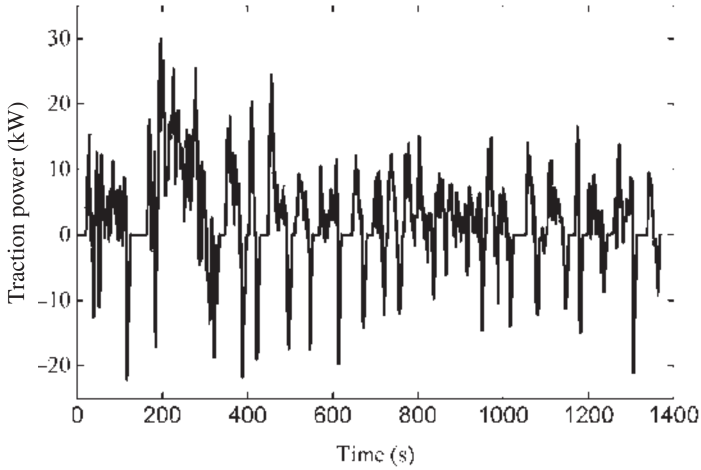

Figure 1.8 Traction power versus time under UDDS.

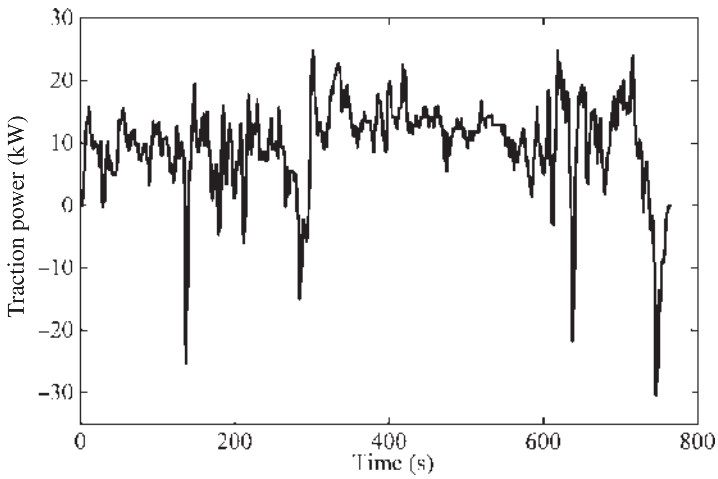

Figure 1.9 Traction power versus time under FHDS.

using Eq. (1.8), and the corresponding results are shown in Table 1.2. In current EV markets, the average size of the battery systems in EVs is around 30 kWh [14, 15]. Thus, it is assumed that the typical PEV has a 30 kWh battery system installed for the evaluation of the range per charge running at the repetitions of the five standard driving cycles until the battery system discharges to 80% of its total energy (i.e. 24 kWh). The corresponding driving distances are shown in Table 1.3.

Generally, an ICEV can easily give a driving range of 480–640 km (i.e. 300–400 miles) with a full tank of gasoline (e.g. 16 gal). For the same driving range, the PEV would require a battery system larger than 100 kWh that weighs over 667 kg, which is too big and heavy. This is due to the fact that gasoline has a theoretical specific energy of

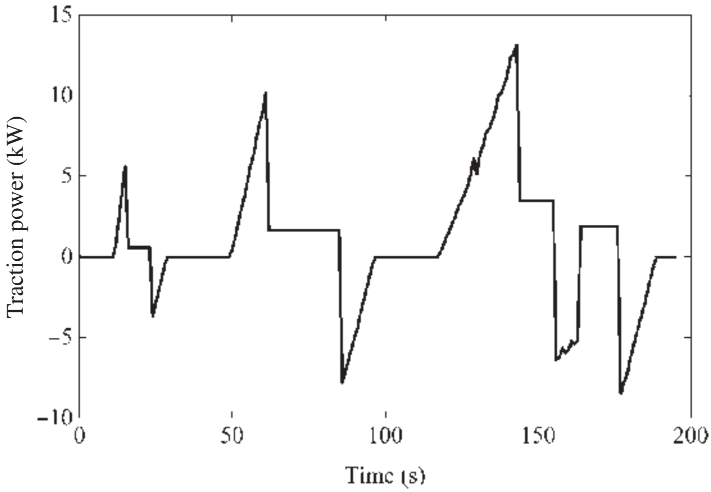

Figure 1.10 Traction power versus time under ECE-15.

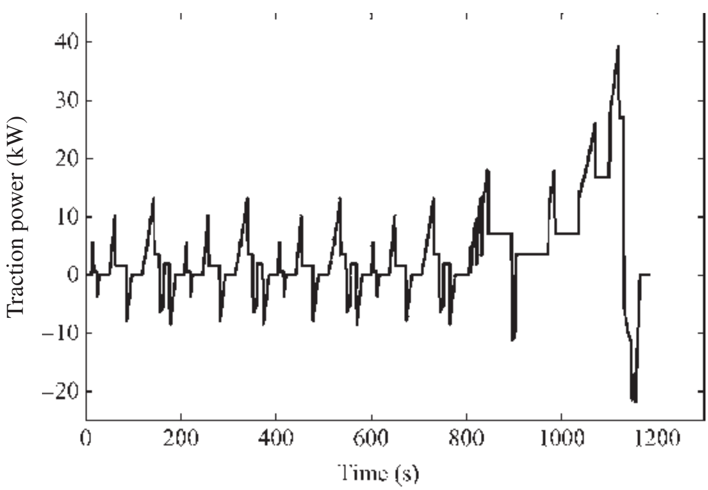

Figure 1.11 Traction power versus time under NEDC.

13 000 Wh kg^{-1}, which is about 100 times higher than the specific energy of 150 Wh kg^{-1} of typical lithium-ion (Li-ion) batteries [16]. However, since the efficiency of a propulsion system in EV powertrains is much higher than that in ICEVs, less energy is needed to propel EVs. Considering the efficiency of the propulsion system is 80% for EVs and 20% for ICEVs, the total amount of energy stored for an EV can be a quarter of what an ICEV needs for the same mileage. Thus, it is realistic to have a battery system of around 30 kWh to achieve around a 200 km (i.e. 124 miles) range based on current battery technologies, where the batteries in EVs are only allowed to discharge to 80% of the total energy (i.e. 24 kWh).

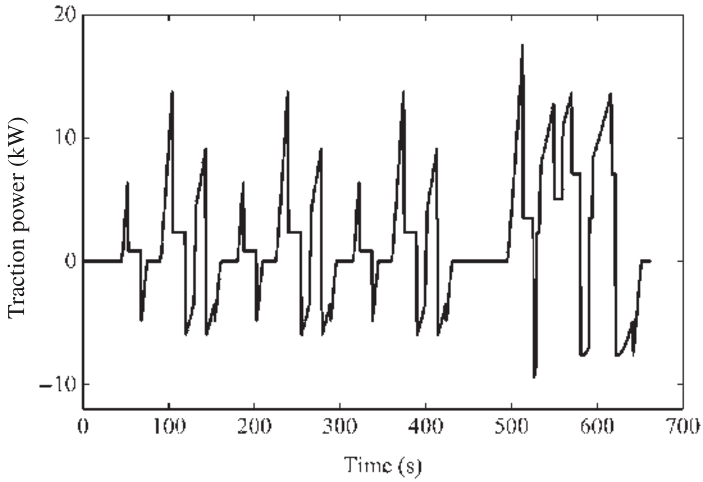

Figure 1.12 Traction power versus time under Japanese 10.15 Mode.

Table 1.2 Energy demands for five standard driving cycles.

	UDDS	FHDS	ECE-15	NEDC	Japanese 10.15
Driving distances (km) per standard driving cycle	11.99	16.51	0.99	10.93	4.17
Energy demands in traction mode, kJ (kWh)	5132 (1.42)	7923 (2.20)	602 (0.17)	5024 (1.40)	1665 (0.46)

Table 1.3 Driving distances for repetition of five standard driving cycles.

	UDDS	FHDS	ECE-15	NEDC	Japanese 10.15
Driving distances without regenerative braking (km)	202	180	140	187	218

1.3.2 Acceleration Rate

The vehicle acceleration is driven by all forces applied on it. This force can be expressed as

$$F_A = M\alpha \tag{1.9}$$

where $\alpha = dV/dt$ is the vehicle acceleration magnitude. The energy required for vehicle acceleration from standstill to a reference speed V_r is calculated by

$$E_A = MV_r^2/2 \tag{1.10}$$

EV batteries provide the energy to accelerate the PEV. If the time t is given for the acceleration process, the relationship between the energy and mean power can be represented approximately by

$$E_A \approx \overline{P}t \tag{1.11}$$

Considering the power increases from zero to the maximum power $P_{\max}$ in the acceleration process, the approximate mean power is

$$\overline{P} \approx P_{\max}/2 \tag{1.12}$$

Substituting Eqs. (1.11) and (1.12) into Eq. (1.10) leads to

$$P_{\max} \approx MV_r^2/t \tag{1.13}$$

If the acceleration rate is expected to be 100 km h^{-1} within 10 seconds for the typical PEV, the maximum power which the batteries need to provide is 104 kW approximately to the discharge rate of 3.5C for the 30 kWh battery system.

1.3.3 Maximum Speed

The maximum speed is an important parameter to indicate EV performance. Since the aerodynamic drag force is the cube of speed, it becomes the dominant factor at high speeds compared with other resistance forces. Thus, the maximum power needed to calculate the maximum speed $V_{\max}$ on a level road with ideal gearing can be simply described as

$$V_{\max} = \sqrt[3]{2P_{\max}/(\rho AC_d)} + V_w \tag{1.14}$$

If the maximum power delivered from the battery system with 30 kWh in the typical PEV is 120 kW which is equivalent to a discharge rate of 4C, then the corresponding maximum speed is found to be 209 km h^{-1} by substituting 120 kW and the parameters in Table 1.1 into Eq. (1.14).

1.4 Battery Systems

Batteries are normally categorized into two types, namely primary and secondary batteries. Primary batteries have non-rechargeable properties and can only be discharged once. These types of batteries are also known as “dry cells.” Secondary batteries have rechargeable properties and can be recharged to their original conditions after discharging. These types of batteries are also known as rechargeable batteries. Battery systems in EVs or PHEVs should provide rechargeable properties with satisfactory performance, including high energy density for covering sufficient driving range, high power density for a vehicle to achieve desired acceleration rate and maximum speed, a long cycle life for minimum maintenance and low cost for better market acceptance. Secondary batteries fulfill most of the above-mentioned criteria and thus are widely used in EVs.

The development of secondary batteries has continued for over 100 years. So far, many different types of secondary batteries have been available in commercial markets. Some of them have been widely used in EVs as energy storage; these are lead–acid, nickel–cadmium (NiCd), nickel–metal hydride (NiMH) and Li-ion batteries [10]. EVs require battery systems to store sufficient energy to meet desired driving distances and provide adequate peak power to deliver a specific acceleration performance. To better understand battery systems in EVs, we first provide an introduction to the electrochemistry of secondary battery cells as the basic building blocks for making battery systems. Then, we present the backgrounds, operating principles, performances and applications of the above-mentioned four types of secondary batteries.

1.4.1 Introduction to Electrochemistry of Battery Cells

Battery cells store energy based on the conversion of chemical energy into electrical energy and vice versa through an electrochemical reaction [16–18]. Figure 1.13 shows a schematic diagram of an electrochemical battery cell. The cell is made up of a negative electrode, a positive electrode, an electrolyte, a separator, a positive current collector, and a negative current collector, and it supplies power to an external load. The solid and porous electrodes allow the electrolyte to pass through. The separator prevents electrons from flowing but allows positive and negative ions to migrate between the two electrodes through the electrolyte. The positive and negative current collectors provide a pathway for electrons to flow through an external load. The cell makes use of the fact that different materials in the positive and negative electrodes immersed in an electrolyte solution have different tendencies to gain and lose electrons.

These electrons will flow through the external load while the resultant ions move in the electrolyte solution, forming a closed circuit to create the current and providing power and energy to the external load. It is convenient to introduce the terms "anode" and "cathode." A cathode is defined as the electrode which accepts electrons from the external circuit or as the electrode at which reduction reaction takes place. Conversely, an anode is defined as the electrode which releases electrons to the external circuit, or as the electrode at which oxidation reaction takes place. The basic working principle of a battery cell is explained below.

During discharge, the positive electrode is the cathode and the negative electrode is the anode. Positive ions flow from the anode to the cathode through the electrolyte and separator. Negative ions flow in the opposite direction. Electrons flow from the anode (negative electrode) to the cathode (positive electrode) through the external load. The anode builds up negative charge and the cathode builds up positive charge, generating a cell voltage V_t. When this voltage is applied across the external load, a current I_t will be produced in the opposite direction of electron flow.

During charge, the process is reversed. The positive electrode is the anode and the negative electrode is the cathode. The positive ions flow from the anode to the cathode through the electrolyte and separator. Negative ions flow in the opposite direction. Electrons flow from the anode (positive electrode) to the cathode (negative electrode) through the external load. The negative electrode material dissolves in the electrolyte solution to form negative ions and gains an electron in what is called the reduction reaction. The positive electrode loses an electron by depositing positive ions from the electrolyte in what is called an oxidation reaction. These oxidation–reduction reactions are reversible in secondary batteries. Thus, batteries can be discharged to return the electrodes to their pre-charged states or charged to their pre-discharged states.

The ions move through the electrolyte under diffusion and migration. Diffusion results from the existence of a concentration gradient in the electrolyte. Over time, if there is no ion production, the ions in the electrolyte diffuse evenly throughout the cell. Migration results from the presence of the electric field generated by the positive and negative

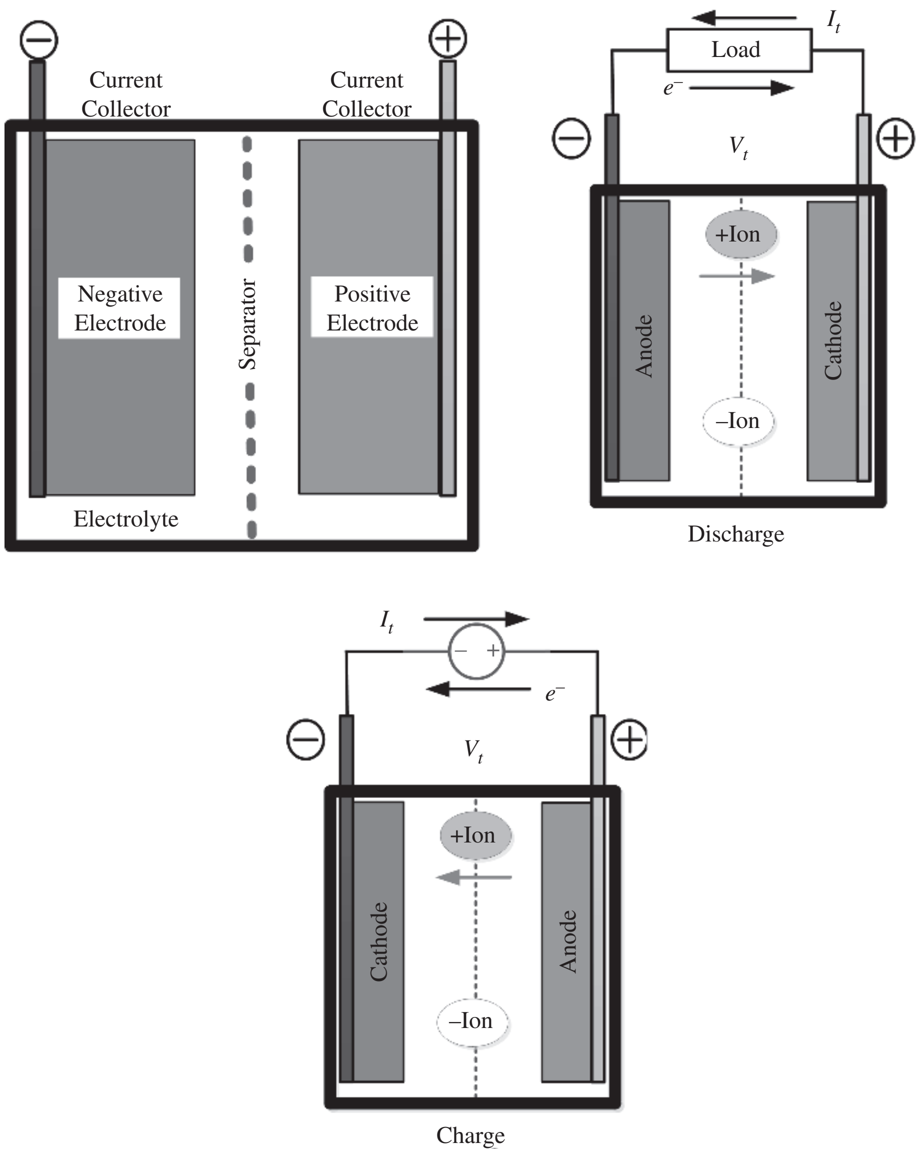

Figure 1.13 Schematic diagram of an electrochemical cell.

electrodes. The positive ions migrate toward the negative electrode and the negative ions migrate toward the positive electrode. The movement of ions through the electrolyte and electrons through the external circuit enables the storage and release of energy.

When the current passes the cell, the cell terminal voltage V_t deviates from its equilibrium state voltage V_{eq}; such deviation is called a polarization voltage or overvoltage η. The polarization voltage incudes three major components:

- Ohmic overvoltage drop which is caused by the resistances in the bulk of the electrolyte, separators, electrodes and current collectors and other connectors.

- Activation overvoltage which is related to the charge transfer at each electrode/electrolyte interface and is also known as "electrode losses."
- Concentration overvoltage which is connected to the depletion or accumulation of active materials near the electrode surface.

In practical batteries, cell voltage for discharging can be expressed as

$$V_t^{dis} = E_{eq} - \eta^{dis} \tag{1.15}$$

while cell voltage undergoes charging

$$V_t^{cha} = E_{eq} + \eta^{cha} \tag{1.16}$$

where η^{dis} and η^{cha} represent the polarization voltages for charging and discharging processes, respectively.

1.4.1.1 Ohmic Overvoltage Drop

The source of ohmic overvoltage drop is the internal resistance of the bulk phases within the cell. If the current distribution is uniform, then for a phase with conductance σ, the resistance is

$$R = x/A\sigma \tag{1.17}$$

where x is the thickness of the phase and A is its cross-sectional area. For the passage of a current I_t through a cell with j sequential phases, Ohmic overvoltage drop is expressed by

$$\eta_{ohmic} = I_t \sum_j (x_j/A_j\sigma_j) \tag{1.18}$$

1.4.1.2 Activation Overvoltage

Activation overvoltage is associated with an electrode process which mainly involves two consecutive steps: (i) the transport of the electroactive species from the bulk of the electrolyte phase to the electrode surface; and (ii) interfacial charge transfer. For relatively low currents, it can be assumed that the surface concentration does not deviate significantly from the bulk value. Hence, the transfer of electrons or ions is the rate-determining step in the process which is directly controlled by potential difference or overvoltage across an electrode/electrolyte interface. The Butler–Volmer equation describes the relationship between electrical current I_t representing the rate of charge transfer and the activation overvoltage η_a as

$$I_t = i_o \left\{ \exp\left(\frac{-\alpha n F \eta_a}{RT}\right) - \exp\left[\frac{-(1-\alpha) n F \eta_a}{RT}\right] \right\} \tag{1.19}$$

where i_o denotes exchange current, α represents the transfer coefficient whose value is a constant between 0 and 1 (typically, it is close to 0.5), F is the Faraday constant, R is the universal gas constant, T is absolute temperature, and n is the number of electrons involved in the electrode reaction.

1.4.1.3 Concentration Overvoltage

For relatively large currents, the transport of electroactive species to the electrode surface becomes the limiting factor to restrict current. Concentration overvoltage η_c is used to describe such current restriction caused by a concentration gradient at the electrode surface. Assuming that diffusion is the only mechanism of transport, the concentration overvoltage can be evaluated using the relationship

$$\eta_c = \frac{RT}{nF} \ln\left(\frac{i_{\text{lim}} - I_t}{i_{\text{lim}}}\right) \tag{1.20}$$

where i_{lim} is a maximum or limiting current corresponding to the maximum concentration gradient.

1.4.2 Lead–Acid Batteries

Lead–acid batteries are the oldest type of secondary batteries and they are used extensively in communication systems, portable devices, heavy industry and EVs as well as stationary applications ranging from small emergency supplies to load leveling in power systems. The initial design of lead–acid batteries is the flooded versions which consist of a negative electrode of porous lead (Pb, lead sponge) and a positive electrode of lead oxide (PbO_2), both immersed in an aqueous solution of sulfuric acid (H_2SO_4). A microporous material as the insulator prevents the two electrodes from touching while allowing the electrolyte and the ions into it to enable conduction. A schematic diagram of a lead–acid battery is shown in Figure 1.14.

The chemical reaction at the positive electrode is

$$\mathrm{PbO_2 + 3H^+ + HSO_4^- + 2}e^- \leftrightarrow \mathrm{PbSO_4 + 2H_2O} \tag{1.21}$$

and that at the negative electrode is

$$\mathrm{Pb + HSO_4^-} \leftrightarrow \mathrm{PbSO_4 + H^+ + 2}e^- \tag{1.22}$$

Thus, the overall chemical reaction is

$$\mathrm{Pb + PbO_2 + H_2SO_4} \underset{\text{charge}}{\overset{\text{discharge}}{\rightleftharpoons}} \mathrm{2PbSO_4 + 2H_2O} \tag{1.23}$$

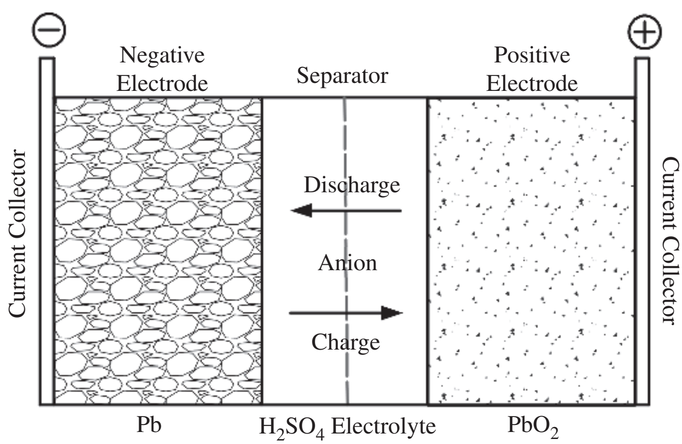

Figure 1.14 Schematic diagram of a lead–acid battery.

According to Eq. (1.23), when the battery is discharged, both electrodes turn into lead sulfate ($PbSO_4$) and the electrolyte loses its sulfuric acid (H_2SO_4) and eventually becomes water. When the battery is charged, the lead sulfate is converted into lead dioxide (PbO_2) at the positive electrode and the sponge lead at the negative electrode, and the electrolyte gains its sulfuric acid. The concentration of the electrolyte increases during the charging process and decreases during the discharging process, thus it can be used to determine the battery's state of charge (SOC).

The valve regulated lead–acid (VRLA) batteries are designed to promote the chemical recombination of the oxygen at the negative electrode to minimize water loss, so they do not require regular checking of the electrolyte level like the flooded lead–acid batteries. VRLA batteries have two forms of immobilized electrolyte: the absorbed electrolyte and the gelled electrolyte in a porous glass separator with voids for oxygen transport. With the immobilized electrolyte, VRLA batteries can reduce evaporation, leakage and vibration problems so that they can be operated in harsh conditions. It is noted that overcharging of lead–acid batteries generates oxygen and hydrogen. Flooded batteries have vents to release the gases and lose water while VRLA batteries recombine them to produce the water within the battery as:

$$2Pb + 2HSO_4^- + 2H^+ + O_2 \leftrightarrow 2PbSO_4 + 2H_2O \tag{1.24}$$

Hence, the water can be recycled in VRLA batteries during overcharge state. This feature leads to VRLA batteries achieving higher charging rate than flooded lead–acid batteries.

1.4.3 NiCd and NiMH Batteries

Nickel-based rechargeable batteries were developed more than 100 years ago. They offer higher performances than VRLA batteries, such as longer cycle life, larger capacity, and faster charging capability. Nickel-based batteries have been widely used in portable devices, telecommunication systems, aircraft and space satellite power systems, military applications, heavy industry and EVs, particularly in hybrid electric vehicles (HEVs). One drawback of nickel-based batteries is that they have relatively high self-discharge rates. The most common nickel-based batteries are NiCd and NiMH batteries .

1.4.3.1 NiCd Batteries

There are different types of NiCd batteries available commercially, such as pocket-plate, sintered-plate and fiber-plate types . The pocket-plate type is the most mature NiCd battery that provides very reliable performance. However, this type is heavy which limits its applications. The sintered-plate type is constructed in a thinner form to reduce battery internal resistance, achieving higher charging and discharging rates. Nevertheless, this type has the drawbacks of manufacturing complexity and high cost. The fiber-plate type uses polymer materials and a plating technique to eliminate most of the drawbacks of its predecessors.

NiCd batteries use nickel hydroxide ($Ni(OH)_2$) as a positive electrode, cadmium (Cd) as a negative electrode and potassium hydroxide solution (KOH) as an electrolyte. The overall chemical reaction is

$$2NiOOH + 2H_2O + Cd \leftrightarrow 2Ni(OH)_2 + Cd(OH)_2 \tag{1.25}$$

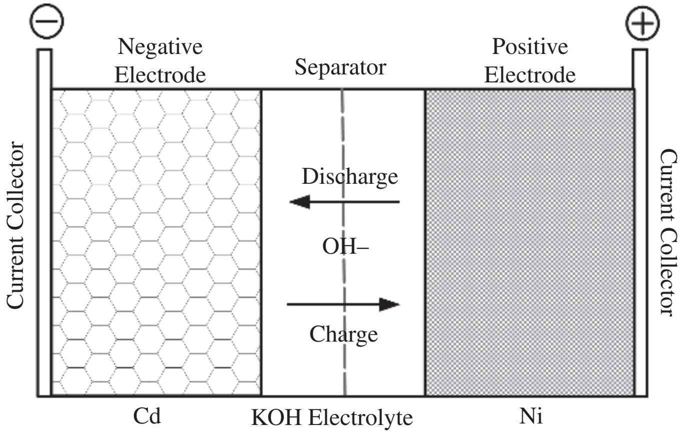

Figure 1.15 Schematic diagram of a NiCd battery.

It can be seen from Eq. (1.25) that metallic cadmium is oxidized to produce $Cd(OH)_2$ while NiOOH is reduced to produce $Ni(OH)_2$ during the discharge process. Figure 1.15 shows a schematic diagram of a NiCd battery. Unlike the sulfuric acid in lead–acid batteries, the concentration of the potassium hydroxide electrolyte in NiCd batteries only changes slightly during the charging and discharging processes and thus cannot be used to determine the SOC. One problem of NiCd batteries is the use of cadmium which has adverse effects on human beings and the environment.

1.4.3.2 NiMH Batteries

NiMH batteries have similar working principles to NiCd batteries. They use a hydrogen-absorbing alloy for a negative electrode instead of cadmium. Without using any cadmium, NiMH batteries are safer and more environmentally friendly. Furthermore, NiMH batteries provide higher energy density and longer cycle life than NiCd batteries. Gradually, NiMH batteries have replaced NiCd batteries in battery markets.

Figure 1.16 shows a schematic diagram of a NiMH cell. The positive electrode contains nickel hydroxide as its principal active material and the negative electrode is mainly composed of hydrogen-absorbing nickel alloys. The cell has an electrically insulating separator, an alkaline electrolyte (e.g. a solution of potassium hydroxide, KOH), and a vented metal case. There are many choices of metal hydride available. The most common ones are AB_2 alloy, a metal alloy of vanadium-titanium-zirconium-nickel and AB_5 alloy, a rare-earth metal alloy of lanthanum-nickel. The electrolyte does not enter into the anode reaction so that conductivity stays at a high level throughout the usable capacity of the battery. In addition, the nickel active material is insoluble in the electrolyte (KOH) which leads to longer life and better abuse tolerance. Only a proton is involved in the charge/discharge reaction, leading to very small changes of electrolyte density and improved mechanical stability of the anode during cycling. The overall chemical reaction for NiMH batteries is

$$MH + NiOOH \leftrightarrow M + Ni(OH)_2 \tag{1.26}$$

Inside NiMH batteries, there is recombination mechanism that allows oxygen to react with hydrogen at the negative electrode, producing water and minimizing the pressure

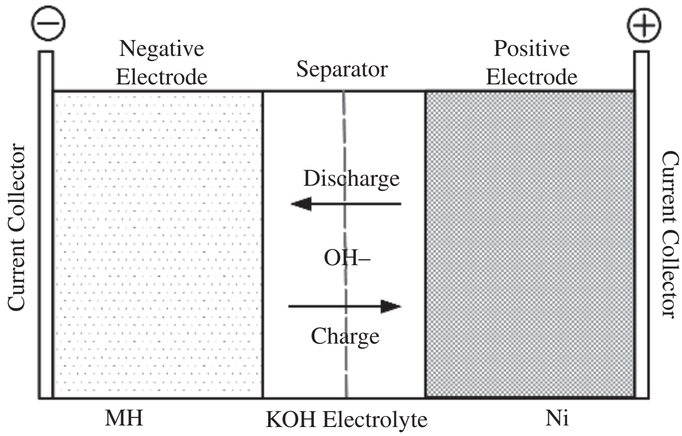

Figure 1.16 Schematic diagram of a NiMH battery.

of the released gases. Note that the charging rate should be controlled to ensure that the generated oxygen does not exceed the recombination rate.

1.4.4 Lithium-Ion Batteries

In order to achieve significant increase in improved energy density and power density, Li-ion batteries have been developed recently. Compared with lead–acid and nickel-based batteries, Li-ion batteries have higher charging and discharging capability, a longer cycle life, and no memory effect. They are very attractive for applications where weight or volume is important, such as mobile phones, laptop computers, and EVs. High initial cost has limited their use in price-sensitive applications, but new chemistries and economies of scale are promising to reduce the cost of Li-ion batteries. For example, large scale Li-ion battery systems have been gradually applied in stationary energy storage in power systems with high penetration of RESs [5].

Li-ion batteries use lithium intercalation compounds as the positive and negative electrodes, where lithium ions move between two electrodes. The negative electrode is deposited onto the copper foil, while the positive electrode, which is a mixture of electroactive material, carbon black and binder, is coated onto the aluminum foil. Both metallic foils ensure the function of the current collector. During discharging, lithium ions are released from the anode (negative electrode) and travel through an organic electrolyte toward the cathode (positive electrode). Electrons flow from the anode to the cathode though the external load. When lithium ions arrive at the cathode, they are quickly inserted into the cathode material. During charging, lithium ions are removed from the cathode for insertion into the anode material. The movement of lithium ions is also known as the intercalation process. Figure 1.17 shows a schematic diagram of a Li-ion battery. Li-ion batteries use materials with a layered structure and a three-dimensional framework structure as the positive electrode. The former includes lithium cobalt oxide (LCO), $LiCoO_2$, and lithium nickel manganese cobalt oxide (NMC), $LiNiMnCoO_2$, while the latter includes the lithium manganese oxide (LMO), $LiMn_2O_4$, and lithium iron phosphate (LFP), $LiFe_2PO_4$. In general, the materials at the negative electrode (anode) are various forms of carbon, particularly graphite and

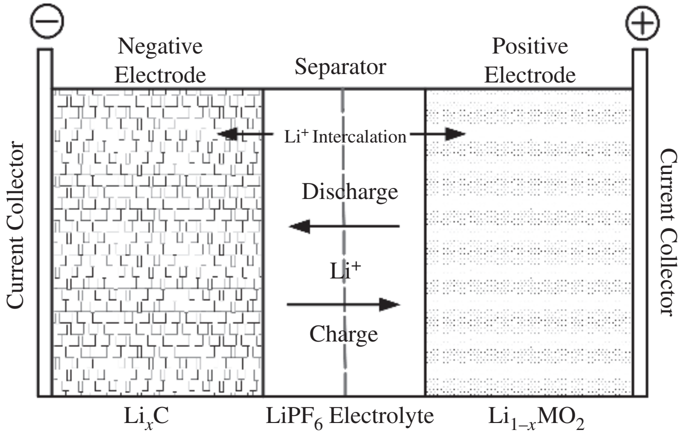

Figure 1.17 Schematic diagram of a Li-ion battery.

hydrogen-containing carbon materials. Different types of carbon electrodes in Li-ion batteries lead to various lithium intercalation capacities and performances. Liquid, gel, polymer or ceramic electrolyte has been adopted in Li-ion batteries. In general, the performance of cobalt oxide is the best among the three types while its cost is much higher than that of nickel oxide and manganese oxide.

There is an exceptional case where the negative electrode uses lithium titanate ($Li_4Ti_5O_{12}$) on the surface of its anode instead of carbon and this type of the battery is known as a lithium titanate battery. Since the lithium titanate battery makes the surface of the negative electrode significantly larger than that with the carbon, it allows electrons to interchange quickly and hence results in a faster charging rate than other types of Li-ion batteries. Its extreme fast charging characteristics will be particularly discussed in Chapter 6.

Although Li-ion batteries consist of different chemical reactions upon various combinations of adopted materials, their overall chemical reaction can be represented by

$$LiYO_2 + C \leftrightarrow Li_xC + Li_{1-x}YO_2 \tag{1.27}$$

where Y represents cobalt, nickel, or manganese. Take Y as cobalt for example, then x depends on the morphology of the cobalt oxide. Despite many advantages, Li-ion batteries are not as safe as lead–acid and nickel-based batteries. Several safety devices with shot-down separator for over temperature, tear-away tab for internal pressure, venting for pressure relief and thermal interruption for overcurrent have to be built into Li-ion batteries.

1.4.5 Battery Performance Comparison

Lead–acid, NiCd, NiMH, and Li-ion batteries have been used as energy sources to power EVs. Their key characteristics in terms of nominal voltage, specific energy and energy density, capacity efficiency and energy efficiency, specific power and power density, self-discharge, cycle life, and temperature operation range are discussed in the following [2, 16].

1.4.5.1 Nominal Voltage

The theoretical voltage of batteries is dependent on the electrode materials used in the batteries. Such a theoretical value may not be able to be achieved in real batteries. Furthermore, the practical voltage of batteries is varied during the charging and discharging processes. The notion of nominal voltage is adopted to define the terminal voltage of rechargeable batteries. The nominal voltage refers to the average value of the working voltage at constant current (CC) during the whole discharging process from a fully charged state to a fully discharged state.

Based on the theoretical voltage of each type of battery, the nominal voltage of a lead–acid cell and a nickel-based cell is defined as 2 and 1.2 V, respectively, and the nominal voltages of Li-ion battery cells are varied from 3.2 to 3.8 V, whilst a LCO has a nominal voltage of 3.6 V, a LMO cell 3.7 (or 3.8) V, a lithium phosphate cell 3.2 V and a lithium titanate cell 2.4 V.

1.4.5.2 Specific Energy and Energy Density

The specific energy is the ratio of the total amount of energy (Wh) stored in the active materials inside a battery cell to the mass of the battery cell (kg). The energy density is the ratio of the total amount of energy (Wh) stored in the active materials inside a battery cell to the volume of the battery cell (l).

Li-ion batteries have the highest specific energy of 250 Wh kg^{-1} which is about 3, 2.6 and 6 times higher than that of NiCd, NiMH and lead–acid batteries, respectively. They also have the highest energy density of 693 Wh l^{-1} which is about 4.6, 2.3 and 6.3 times higher than that of NiCd, NiMH and lead–acid batteries, respectively.

1.4.5.3 Capacity Efficiency and Energy Efficiency

The ability of batteries to accept charge or be recharged is measured in terms of the coulombic efficiency and the energy efficiency of the charge/discharge cycle. The coulombic efficiency is defined as

$$\mu_c = \int_0^{t_{dis}} i_{dis} dt \Big/ \int_0^{t_{cha}} i_{cha} dt \tag{1.28}$$

where t_{dis} and t_{cha} are the total discharge and charge times, respectively, and i_{dis} and i_{cha} are the battery currents flowing during the discharging and charging processes, respectively. The energy efficiency is defined as

$$\mu_e = \int_0^{t_{dis}} v_{dis} i_{dis} dt \Big/ \int_0^{t_{cha}} v_{cha} i_{cha} dt \tag{1.29}$$

where v_{dis} and v_{cha} are the battery voltages during the discharging and charging processes, respectively.

Since the voltage in the charging process is higher than that in the discharging process, energy efficiency is lower than capacity efficiency. For example, the energy efficiency of Li-ion batteries is generally around 85–95% and their capacity efficiency is near to 100%.

1.4.5.4 Specific Power and Power Density

The specific power is the ratio of the rated power (W) which can be delivered from a battery cell to the mass of the battery cell (kg). The power density is the ratio of the rated power (W) which can be delivered from a battery cell to the volume of the battery cell (l). They both indicate how quickly the batteries can provide the necessary energy to loads or how much energy the batteries can deliver in a particular time. Li-ion batteries have the highest specific power and power density, followed by NiMH and then NiCd batteries; lead–acid batteries are the least powerful.

1.4.5.5 Self-discharge

Self-discharge is caused by internal chemical reactions. It reduces the stored charge of batteries even when batteries are not in use. All batteries have internal leakage (self-discharge) and the leakage increases with temperature. Li-ion batteries and lead–acid batteries both have a self-discharge rate of 5% per month compared with 10% per month for NiCd batteries and 20% per month for NiMH batteries.

1.4.5.6 Cycle Life

The cycle life is the number of charge/discharge cycles that can be achieved before a battery reaches the end of its useful life. In EVs, the end of useful life is defined as a capacity drop to 80% of the original capacity. Cycle life depends mainly on battery temperature, discharge profile and depth of discharge (DOD). In general, batteries have longer life for low DOD cycles. For example, Li-ion batteries typically last 2000 cycles at low discharge/charge rates and room temperature at 100% DOD; they can last up to 20 000 cycles at 20–40% DOD.

1.4.5.7 Temperature Operation Range

Batteries perform poorly at extremely low and high temperatures. Low temperatures hinder ionic diffusion and migration and lead to damaging side reactions (e.g. lithium plating). High temperatures cause other side reactions, such as corrosion and gas generation. For lead–acid batteries, charge and discharge temperatures should be limited to an operation range of −15 to 50 °C. Li-ion batteries have an operation range of −20 to 60 °C. NiCd and NiMH batteries have operation ranges of −20 to 50 °C and −20 to 60 °C, respectively.

Table 1.4 shows the comparison of lead–acid, NiCd, NiMH and Li-ion batteries. It can be seen that Li-ion batteries have advantages over the other three types of batteries in almost all aspects. Furthermore, most EVs today use Li-ion batteries [14, 15]. Thus, the focus will be on advanced BMSs for Li-ion batteries for the remainder of the book.

1.5 Key Battery Management Technologies

The development of advanced BMSs for EVs involves many technologies due to the complicated electrochemical reactions and diversity of the cells in the battery system as well as their performance degradation over time. In the following, the key BMTs will be discussed. They include battery modeling, battery states estimation, battery charging, and battery balancing [2, 8, 9].

1.5.1 Battery Modeling

Battery modeling forms the foundation for the design, control and optimization of BMSs in EVs. It has a significant impact on the estimation of battery states, battery balancing,

Table 1.4 Comparison of four types of batteries in EVs.

	Lead–acid	NiCd	NiMH	Li-ion
Specific energy (Wh kg^{-1})	33–42	50–80	70–95	118–250
Energy density (Wh l^{-1})	60–110	50–150	140–300	250–693
Specific power (W kg^{-1})	180	200	200–300	200–430
Power density (W l^{-1})	450	200	300	800
Nominal voltage (V)	2	1.20	1.20	3.6
Overcharge tolerance	High	Moderate	Low	Very low
Self-discharge (per month)	<5%	10%	20%	<5%
Operating temperature (°C)	−15 to 50	−20 to 50	−20 to 60	−20 to 60
Cycle life	500 ~ 1000	2000	<3000	2000
Energy efficiency	>80%	75%	70%	85–95%

battery charging, and battery fault diagnosis. Over the years, numerous battery models have been developed to describe battery behaviors. All these models can be mainly categorized into three groups: electrochemical models; blackbox models; and equivalent circuit models.

Electrochemical models provide a highly accurate description of electrochemical processes inside a battery. The models involve many partial differential equations (PDEs). Solving these PDEs leads to large computation burden overhead. Furthermore, many battery electrochemistry related parameters in PDEs are practically difficult to acquire in EVs. In general, electrochemical models are suitable for battery design and simulation but are not appropriate for real-time BMSs in EVs.

Blackbox models apply artificial intelligence (AI) techniques to capture the relationship between the selected inputs and outputs of batteries without the prior knowledge of electrochemical processes inside batteries. AI techniques such as neural network (NN) [19], fuzzy logic (FL) [20], and support vector machine (SVM) [21] apply training approaches to establish the models based on testing data. To achieve high model accuracy and good generalization ability, testing data should cover sufficient battery operation ranges, and the parameters in the training approaches need to be effectively tuned.

Equivalent circuit models describe battery behaviors using a combination of the lumped circuit parameters, such as resistances, capacitances and voltage or current sources. Due to their simple model structure and relatively small number of model parameters, the models are widely adopted in real-time BMSs for EVs, where overall dynamic characteristics of battery terminal voltage, current, temperature, and SOC are of more interest than the detailed electrochemical reactions inside batteries. Furthermore, equivalent circuit models are more intuitive and can be easily incorporated in the electrical circuits in BMSs. Thus, the focus of this book is on the equivalent circuit models. Chapter 2 will provide detailed discussions of battery modeling techniques.

1.5.2 Battery States Estimation

Battery states are crucial for BMSs to monitor and protect batteries and optimize the operation of batteries. Many battery parameters can indicate battery states. The discussions will be on the key states used in BMSs, including SOC, state of energy (SOE), state of power (SOP), and state of health (SOH).

The SOC is the ratio of the remaining capacity to the nominal capacity of the battery. Similarly, the SOE is the ratio of the remaining energy to the nominal energy of the battery. They are both often expressed as a percentage. If the battery is fully charged, the SOC (or SOE) is known as 100%; if the battery is fully discharged, the SOC (or SOE) is defined as 0%. Numerous methods are developed for SOC (or SOE) estimation. Generally, they are categorized as direct estimation methods and model-based estimation methods. For the direct estimation methods, the SOC (SOE) can be calculated by Ampere-hour (Ah) counting and open circuit voltage (OCV) at battery equilibrium state. For the model-based estimation methods, they can be further divided into two groups. In the first group, electrochemical models and equivalent circuit models are usually represented in the form of state space equations, where the SOC (or SOE) is one of the state variables. Then, state observers are adopted for the SOC (or SOE) estimation, such as Kalman filters (KFs) and their variants, sliding mode observers, and H infinite filters. In the second group, blackbox models are used to directly establish the relationship between the measurable battery parameters (i.e. voltage, current, and temperature) and the SOC (or SOE) based on testing data through training approaches, such as NN, FL and SVM models. Chapter 3 is devoted to presenting the SOC and SOE estimation approaches in detail.

The SOH is the ratio of the capacity of the aged battery to the nominal capacity of the new battery. It is also expressed as a percentage. For the new battery, the SOH is defined as 100%. When the SOH falls to 80%, it is defined as the end of the battery life for EVs. However, EV batteries at a SOH of 80% may be able to be reused as stationary energy storage. Numerous methods have been proposed to estimate the SOH; they are categorized as the model-free estimation method, the model-based estimation method, and the data-driven estimation method. For the model-free estimation method, the standard capacity test is conducted to measure the aged battery capacity in each charge and discharge cycle. According to the definition of the SOH, it can be calculated by dividing the measured capacity by the nominal capacity. For the model-based estimation method, they can be further divided into two groups. In the first group, battery capacity is taken as a slow time-varying parameter based on equivalent circuit models [22] and electrochemical models [23]. Various observer techniques such as KFs and their variants and sliding mode observers are adopted to estimate the capacity for the calculation of the SOH. In the second group, battery life-cycle and aging models are developed to estimate the capacity degradation and predict the battery life cycle [24]. For the data-driven estimation method, AI techniques are employed to analyze the measured battery parameters such as battery terminal voltage, current, and temperature in real time for the SOH estimation; these AI techniques include SVM, NN, Naive Bayes, Bayesian learning and Bayesian Monte Carlo methods [25]. There is another way to calculate the SOH based on the ratio of the internal resistance of the aged battery to the internal resistance of the new battery. The above-mentioned model-free, model-based and data-driven methods can also be used to estimate the SOH in terms of battery internal resistance. The details of the SOH estimation approaches are discussed in Chapter 4.

The SOP is defined as the ratio of peak power to nominal power. The accurate estimation of peak power in BMSs is critical in EVs since it is necessary to determine power available at the moment to meet acceleration, regenerative braking and gradient climbing power requirements without overcharging or over-discharging batteries [26]. More importantly, the SOP can be used to optimize the relationship between battery capacity and EV performances. Many SOP methods are developed for EVs. They can be divided into four types. The first type is the hybrid pulse power characterization (HPPC) method. When the HPPC method is applied to estimate the SOP, it only considers operation voltage limits while estimating peak power and instantaneous current. The second type is the SOC-limited method. It takes into account the maximum and minimum operation SOCs of a battery. Generally, it provides an optimistic prediction of peak current to be discharged or charged over a wide range of the SOC. The third type is the voltage-limited method. It is suitable for continuous peak power estimation while neglecting the SOC limits. The fourth type is the multi-constraint dynamic method. This method estimates peak power under the constraints of its voltage, current, temperature, available capacity, and SOC. The relaxation effect is also considered in this method. Chapter 5 is devoted to discussing the details of SOP estimation approaches.

1.5.3 Battery Charging

Battery charging plays an important role in the wide adoption of EVs. It will refill the battery system on its depletion. The issues on battery charging involve charging time, power transfer and charging facilities, and charging algorithm. Among them, the charging algorithm is crucial to battery charging. It defines a charging profile to charge the battery system in terms of current and voltage over time and a condition to terminate the charging process. The charging profile of CC is normally used to charge NiCd/NiMH batteries, whereas the charging profile of constant voltage (CV) is normally used to charge lead–acid batteries. For Li-ion batteries, many charging algorithms have been developed, including constant current constant voltage (CC/CV), multistep constant current (MSCC), two-step constant current constant voltage (TSCC/CV), constant voltage constant current constant voltage (CVCC/CV), pulse current (PC), and pulse voltage (PV) [18]. Recently, there have been two new developments in charging Li-ion batteries. One was to find the optimal charging current profile for Li-ion batteries and the other was to develop a Li-ion battery with extremely fast charging and discharging capability.

For the termination of a charging process, SOC is an ideal indicator to stop charging a battery when the SOC reaches 100%. However, the SOC is not a directly measured parameter. The accurate estimation of the SOC is a very challenging task. Even if the SOC can be estimated accurately, backup methods are still required to stop a charging process using the directly measured parameters, such as voltage, current, or the temperature of a battery. Different techniques have been proposed to stop the charging process in terms of battery electrochemical characteristics. The voltage drop (ΔV) is normally incorporated with the CC to stop charging NiCd/NiMH batteries, whereas the cut-off current is normally incorporated with the CV to stop charging lead–acid and Li-ion batteries. There are many other termination techniques, such as timer, temperature cut-off, temperature change rate (dT/dt), cut-off voltage for charge, cut-off voltage for discharge and voltage change rate (dV/dt). Chapter 6 discusses battery charging techniques in detail.

1.5.4 Battery Balancing

Battery systems generally consist of hundreds and thousands of battery cells connected in series and parallel to fulfill voltage, power and energy requirements for EVs. An imbalance of the serially connected cells in battery systems occurs inevitably after a few charge and discharge cycles and deteriorates over time. The imbalanced conditions can cause overcharging or over-discharging cells, prevent the full utilization of battery capacity and reduce lifecycle of battery systems. Battery balancing is required to equalize voltage, SOC and capacity of all cells in battery systems to maintain their performances [27].

Battery system imbalance can be capacity imbalance, SOC imbalance, and voltage imbalance. Capacity imbalance takes place in the aged battery system. It mainly results from different aging speeds of the cells which are strongly affected by the charging and discharge current, DOD, and ambient temperature. SOC imbalance takes place in the fresh battery system. It is caused by different charging and discharge efficiencies and self-discharge rates of the cells. Voltage imbalance takes place in the battery system at any time. It is caused by cell capacity divergences and different internal parameters such as internal resistance.

There are two categories of battery balancing methods. One category is the passive balancing method. It equalizes the battery system by dissipating the energy from cells into heat through the shunting resistor and is only effective in the charging process to help fully charge all the cells in the battery system. The other category is the active balancing method. It equalizes the battery system by transferring the energy among cells in the battery system through power electronic circuits and can be used in both charging and discharging processes to help fully charge and discharge all the cells in the battery system. Chapter 7 gives a detailed discussion of battery balancing techniques.

1.6 Battery Management Systems

The capacity and voltage of a single battery cell is relatively low. A battery system is required in EVs. The battery system consists of hundreds and thousands of single cells connected in series and parallel, where the series connection of cells yields a higher total battery voltage at the same capacity and the parallel connection of cells yields a higher total battery capacity at the same battery voltage. To manage such a large number of battery cells, a BMS is highly desirable, which should have an ability to maintain the health of all the cells to deliver the power and energy as required by EVs through monitoring and controlling the cells, estimating battery states, balancing the cells, and reporting the status of the cells in battery systems [7–9].

The BMS in EVs consists of many sensors, actuators, and controllers embedded with models and algorithms. The main tasks of the BMS are as follows:

- Monitor and measure the parameters of all the cells in battery systems.
- Protect the battery system to ensure its safe and reliable operation.
- Maintain all the cells within the manufacturer-recommended operating conditions to prolong the life of the battery system.
- Optimize the energy usage of the battery system.
- Communicate to other units and the vehicle control unit (VCU).

These tasks are implemented by the hardware and software built in the BMS.

1.6.1 Hardware of BMS

The major hardware circuits of the BMS include: (i) current, voltage and temperature sensors to measure battery parameters. (ii) Battery state estimators to estimate battery states, such as SOC and SOH. (iii) On-board fault diagnosis to detect the faults including sensor fault, actuator fault, communication network fault, battery fault, loose connection, exceeding combustible gas concentration, insulation fault, uniformity fault, over-fast temperature rise fault, and provide the warning signals of these faults. (iv) Battery protection circuits to prevent the battery system from overcharging, over-discharging, overcurrent, ultra-high temperature, and ultra-low temperature. When the corresponding threshold values are exceeded the error messages are provided to alert EV drivers and correspondingly the safety switches execute protection commands. (v) Battery passive or active equalization circuits (equalizers) to balance the voltages or SOCs or capacities among the cells as consistent as possible. (vi) Battery charger to charge the battery system based on the predefined charging algorithm. (vii) Thermal controller to start the heater or fan during battery charging or discharging processes. (viii) Communication unit to transfer measured data and conduct on-line calibrating, monitoring, automatic code generation, and program downloading. (ix) Information storage unit to store key data, such as SOC, SOH, internal resistance, maximum and minimum voltage and temperature, accumulated charge and discharge ampere hours, fault code and uniformity.

1.6.2 Software of BMS

The software of the BMS is considered as a "brain" which will control the operation of the hardware, make decisions, and estimates states. It includes: (i) battery models to represent the cell and battery system. (ii) Estimation algorithms for battery states, such as SOC (SOE), SOH, and SOP. (iii) Fault diagnosis algorithms to detect different types of faults. (iv) Control algorithms to control the thermal system in terms of the normal range of working temperatures and the safety switches in terms of the range of normal working voltages. (v) Charging algorithms to decide the level of voltage and current to charge the battery systems. (vi) Battery balancing algorithms to equalize the battery cells based on battery terminal voltage or SOC or capacity as a balancing criterion. (vii) Communication protocols to control the data flows within the BMS and to exchange the data with VCU and other parts of EVs including a power inverter/charger, environmental control units (e.g. fans and heaters). Figure 1.18 illustrates the functional blocks of BMSs for EVs.

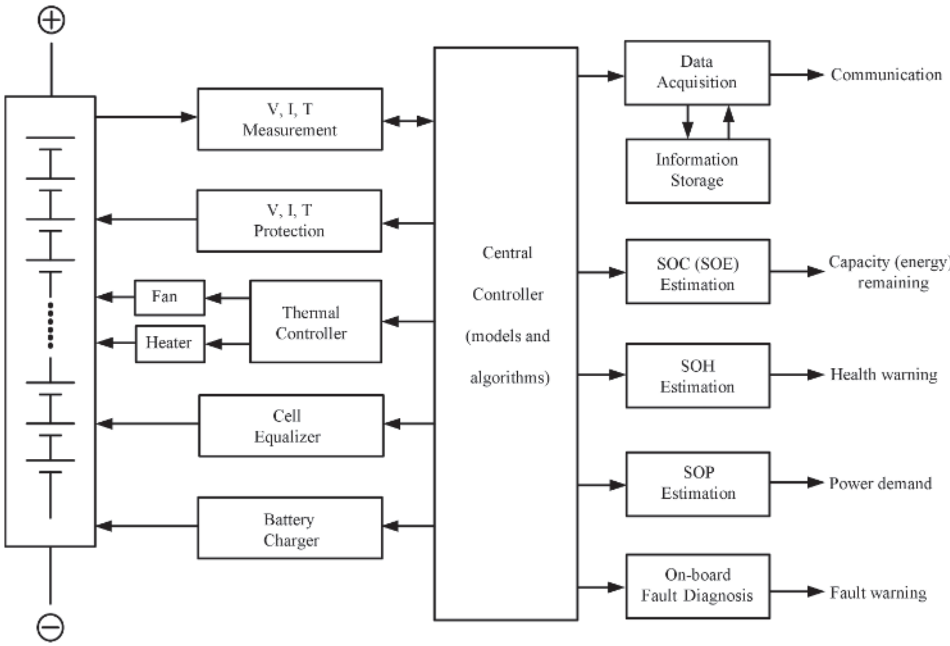

Figure 1.18 Battery management system for EVs.

To explain how these blocks work together, the process of battery charging in the BMS is taken as an example. During the charging process, the measurement block converts the currents, voltages, and temperatures of each cell in the battery system into digital signals. These measured parameters are sent to the state estimation block to estimate SOC and SOH and to the thermal system to heat up or cool the battery systems. The estimated SOC and SOH are sent to the battery cell equalizer and charge controller for the calculation of balancing and charging currents and charging voltage based on the battery model. The equalizer and charge controller generate the control signals of the balancing currents, charging currents, and charging voltage for the charger to perform cell balancing while charging the battery systems according to a pre-selected charging algorithm such as the constant current constant voltage charging algorithm. Once the battery system is fully charged in terms of the preset charging termination parameters, such as 100% SOC or the upper cut-off battery, the safety switches are turned off to protect the battery system from overcharging. The communication block is responsible for transferring the data related to the charging algorithm inside the BMS.

There are a number of different BMS architectures depending on the number of cells in the battery system and its physical structure. These architectures are mainly classified into two categories [28]: the centralized BMS and the distributed BMS.

1.6.3 Centralized BMS

The centralized BMS is a single controller board to monitor and control all the cells in the battery system. It requires extensive wiring from all the cells to the controller board and thus can hardly be scaled up. The centralized BMS is the most economical architecture and is suitable for a battery system with a small number of cells.

1.6.4 Distributed BMS

The distributed BMS has a combination of many slave boards and a master board. A slave board measures and controls an individual cell in the battery system. The slave boards are interconnected via a serial network and controlled by the master control board. A distributed BMS architecture is much easier to install than a centralized one. For a battery system with a large number of cells, the cost of a distributed system can be significantly higher than for a centralized system.

Chapter 8 will describe the structure of the BMS, its representative products and the key technologies in the future generation of the BMS.

1.7 Summary

This chapter describes EV fundamentals including the concepts of traction force, aerodynamic drag force, rolling resistance force and climbing force applied to EVs, focusing on the derivation of governing equations of EV motion. Based on these equations, the power and energy demands of EV batteries are discussed in terms of EV driving range per charge under standard driving cycles, acceleration rate, and maximum speed.

Then, an introduction to electrochemistry of batteries is provided to lay the foundation to explain the working principles of the most common batteries in EVs: lead–acid, NiCd, NiMH, and Li-ion batteries. The performances of these batteries are compared and discussed.

Finally, the key BMTs including battery modeling techniques, battery SOC, SOE, SOH and SOP estimation approaches and their implementation in BMS are briefly presented. The compositions, functions and architectures of the BMS are also discussed.

References

1 Chan, C.C. (2007). The state of the art of electric, hybrid, and fuel cell vehicles. *Proceedings of the IEEE* 95 (4): 704–718.
2 Kumar, M.S. and Revankar, S.T. (2017). Development scheme and key technology of an electric vehicle: an overview. *Renewable and Sustainable Energy Reviews* 70: 1266–1285.
3 Chrisafis, A. and Vaughan, A. (2017) France to ban sales of petrol and diesel cars by 2040. https://www.theguardian.com/business/2017/jul/06/france-ban-petrol-diesel-cars-2040-emmanuel-macron-volvo (accessed 24 April 2018).
4 *The Economist* (2017) China moves towards banning the internal combustion engine. https://www.economist.com/news/business/21728980-its-government-developing-plan-phase-out-vehicles-powered-fossil-fuels-china-moves (accessed 24 April 2018).
5 Garcia-Valle, R. and Pecas Lopes, J.A. (2013). *Electric Vehicle Integration into Modern Power Networks, Power Electronics and Power Systems*. New York: Springer.

6 Deng, J., Li, K., Laverty, D.M. et al. (2014). Li-ion battery management system for electric vehicles-A practical guide. In: *International Conference on Life System Modeling and Simulation and International Conference on Intelligent Computing for Sustainable Energy and Environment*, 32–44. Springer.

7 Rahimi-Eichi, H., Ojha, U., Baronti, F., and Chow, M.Y. (2013). Battery management system, an overview of its application in the smart grid and electric vehicles. *IEEE Industrial Electronics Magazine* 7 (2): 1–16.

8 Hannan, M.A., Lipu, M.S.H., Hussain, A., and Mohamed, A. (2017). A review of lithium-ion battery state of charge estimation and management system in electric vehicle applications: challenges and recommendations. *Renewable and Sustainable Energy Reviews* 78: 834–854.

9 Lu, L., Han, X., Li, J. et al. (2013). A review on the key issues for lithium-ion battery management in electric vehicles. *Journal of Power Sources* 226: 272–288.

10 Chau, C.C. and Chau, K.T. (2001). *Modern Electric Vehicle Technology*. Oxford: Oxford University Press.

11 Zhang, X. and Mi, C. (2001). *Vehicle Power Management, Modeling, Control and Optimization*. London: Springer.

12 Wikipedia (2018) Driving cycle. http://en.wikipedia.org/wiki/Driving_cycle (accessed 24 April 2018).

13 Giakoumis, E.G. (2017). *Driving and Engine Cycles*. Cham, Switzerland: Springer.

14 Berckmans, G., Messagie, M., Smekens, J. et al. (2017). Cost projection of state of the art lithium-ion batteries for electric vehicles up to 2030. *Energies* 10: 1314.

15 Grunditz, E.A. and Thiringer, T. (2016). Performance analysis of current BEVs-based on a comprehensive review of specifications. *IEEE Transactions on Transportation Electrification* 2: 270–289.

16 Rahn, C.D. and Wang, C.Y. (2013). *Battery Systems Engineering*. Chichester: Wiley.

17 Berndt, D. (1997). *Maintenance-Free Batteries-Lead-Acid, Nickel/Cadmium, Nickel/Metal Hydride a Handbook of Battery Technology*, 2e. Taunton: Research Studies Press Ltd.

18 Chau, K.T. (2016). *Energy Systems for Electric and Hybrid Vehicles*. London: The Institution of Engineering and Technology.

19 Shen, W.X., Chan, C.C., Lo, E.W.C., and Chau, K.T. (2002). A new battery available capacity indicator for electric vehicles using neural network. *Energy Conversion and Management* 43 (6): 817–826.

20 Chau, K.T., Wu, K.C., Chan, C.C., and Shen, W.X. (2003). A new battery capacity indicator for nickel–metal hydride battery powered electric vehicles using adaptive neuro-fuzzy inference system. *Energy Conversion and Management* 44 (13): 2059–2071.

21 Wang, J., Chen, Q., and Cao, B. (2006). Support vector machine based battery model for electric vehicles. *Energy Conversion and Management* 47 (7): 858–864.

22 Xiong, R., Sun, F., and He, H. (2016). Model-based health condition monitoring method for multi-cell series-connected battery pack. In: *IEEE Transportation Electrification Conference and Expo (ITEC)*, 1–5. IEEE.

23 Xiong, R., Li, L., Li, Z. et al. (2018). An electrochemical model based degradation state identification method of lithium-ion battery for all-climate electric vehicles application. *Applied Energy* 219: 264–275.

24 Zhang, Y., Xiong, R., He, H., and Pecht, M. (2018). Lithium-ion battery remaining useful life prediction with Box-Cox transformation and Monte Carlo simulation. *IEEE Transactions on Industrial Electronics* https://doi.org/10.1109/TIE.2018.2808918.

25 Zhang, Y., Xiong, R., He, H., and Pecht, M. (2018). Long short-term memory recurrent neural network for remaining useful life prediction of lithium-ion batteries. *IEEE Transactions on Vehicular Technology* https://doi.org/10.1109/TVT.2018.2805189.

26 Sun, F., Xiong, R., and He, H. (2014). Estimation of state-of-charge and state-of-power capability of lithium-ion battery considering varying health conditions. *Journal of Power Sources* 259: 166–176.

27 Cu, X., Shen, W.X., Zhang, Y. et al. (2016). Novel active $LiFePO_4$ battery balancing method based on chargeable and dischargeable capacity. *Computers and Chemical Engineering* 97: 27–35.

28 Bingeman, M. and Ben Jeppesen, N. B. (2016) Improving battery management system performance and cost with Altera FPGAs. WP-01247-1.1, Altera Corporation.